coatings

MDPI

Article

Enhancing Surface Integrity and Fatigue Performance of 42CrMo Rolled Threads Through Localized Root Rolling Strengthening

Ziliang Huang [1], Shiqi Chen [1,*], Zhilong Xu [1], Fasheng Zhong [2], Zejie Li [1], Weiwen Chen [1], Qingshan Jiang [1] and Bicheng Guo [1]

[1] College of Marine Equipment and Mechanical Engineering, Jimei University, Xiamen 361021, China; 13357795226@163.com (Z.H.); zhilong.xu@163.com (Z.X.)
[2] Xiamen XGMA CREC Heavy Machinery Co., Ltd., Xiamen 361023, China
* Correspondence: chensq_17@163.com

Abstract

To improve the fatigue life of high-strength bolts, this study builds upon conventional thread rolling by introducing a localized rolling reinforcement process specifically at the thread root. Experimental specimens were prepared from 42CrMo high-strength bolts using a combined manufacturing technique that integrates thread forming and root rolling. A comparative analysis was conducted to evaluate the fatigue performance of bolts with and without the root rolling reinforcement. The experimental results demonstrated that the thread root rolling treatment further refines the surface grains beyond the effects of standard thread rolling. At a rolling force of 2.5 kN, the surface microhardness increased from the original 500 HV0.2 to 540 HV0.2. The process also improved surface finish, reduced grain size, and increased dislocation density. The optimal enhancement was achieved at a rolling force of 3.5 kN, resulting in an approximately 11-fold improvement in fatigue life. Fractographic analysis via Scanning Electron Microscopy (SEM) indicated a reduced number of crack initiation sites. This study confirms the effectiveness of the proposed rolling reinforcement process, offering a viable technical pathway for optimizing the anti-fatigue manufacturing of high-strength bolts.

Keywords: 42CrMo high-strength bolt; thread rolling; localized root rolling strengthening; surface integrity; fatigue performance

Check for updates

Academic Editors: Chithirai Pon Selvan, Avinash Lakshmikanthan and Wahidul K. Biswas

Received: 23 December 2025
Revised: 6 January 2026
Accepted: 9 January 2026
Published: 11 January 2026

Copyright: © 2026 by the authors. Licensee MDPI, Basel, Switzerland. This article is an open access article distributed under the terms and conditions of the Creative Commons Attribution (CC BY) license.

1. Introduction

High-strength bolts are critical load-bearing connecting elements in modern high-end equipment, and their reliability directly determines the safe operation of entire systems. In the wind power sector, thousands of high-strength bolts are relied upon for crucial connections such as those between blades and pitch bearings and for connecting massive tower sections [1,2]. Similarly, in aerospace, high-speed rail, and major industrial equipment, bolts serve as primary force-bearing components in structural joints [3,4]. However, the thread root of high-strength bolts, due to its inherent V-notch geometry, is highly susceptible to becoming a fatigue crack initiation site under cyclic loading. Statistics indicate that approximately 65%–70% of fatigue failures in bolts originate from the thread root [5,6]. Therefore, effectively improving the fatigue performance of the thread root in high-strength bolts has become a major focus of international research.

Rolled threads have garnered significant attention due to their advantages in fatigue strength, surface integrity, and material utilization [7,8]. Compared to traditional cutting or

extrusion forming processes, thread rolling is a cold plastic working technique. It can create continuous metal flow lines in the threaded region and introduce beneficial compressive residual stresses in the surface layer. Consequently, it enhances the bolt's fatigue life, anti-loosening performance, and resistance to stress corrosion cracking, while avoiding defects like micro-cracks or fiber cutting that can arise from machining [9,10]. For instance, addressing the difficulty in cold rolling Ti6Al4V titanium alloy threads and high tool wear, Jiang et al. [11] proposed a novel warm rolling process combining medium-frequency induction heating with axial feed. Through finite element simulation and experimental verification, they found the optimal forming temperature to be 800 °C, under which the rolling torque was reduced by 74% compared to cold rolling, and thread dimensional accuracy was improved. Their study further revealed the metal flow during warm rolling and confirmed that the formed threads obtained a dense and directionally aligned microstructure, with overall hardness significantly increased—the maximum surface hardness was about 35% higher than the substrate. Wang et al. [12] systematically analyzed the influence of different feed times on the gradient microstructure and hardness distribution of Ti6Al4V threads. Zhang et al. [13] investigated the effect of the axial feed rolling process on the surface and sub-surface properties of threaded parts, indicating that using MoS_2 grease and increasing rolling speed helped improve surface quality and reduce roughness. Lu et al. [14] employed a warm rolling process to form threads on the high-strength material GH4169. High-cycle fatigue tests showed its fatigue life was increased by 20–25 times compared to traditionally machined specimens. Although research on rolled threads is relatively mature, conventional thread rolling is a bulk forming process applied to the entire bolt, whereas fatigue failure often originates from localized stress concentration at the thread root. Therefore, it remains necessary to further strengthen this specific area through targeted surface modification techniques.

Surface modification techniques typically utilize high-energy-density input to induce severe plastic deformation in the material's surface layer, thereby enhancing surface strength and fatigue performance [15,16]. Currently, most research focuses on strengthening the thread roots of machined bolts [17]. For example, Wang et al. [18] applied deep rolling to the thread roots of machined bolts. Their results showed that the method introduced a beneficial compressive residual stress field, effectively mitigating tensile stresses. Cheng et al. [19] used ultrasonic rolling to strengthen machined thread roots, achieving greater plastic deformation depth and a more significant residual stress field, resulting in approximately a 3-fold increase in bolt fatigue life. Wang et al. [20] developed a double-roller bilateral synchronous rolling process and systematically characterized the resulting modified surface layer. These studies demonstrate that rolling reinforcement applied to thread roots can effectively improve bolt fatigue performance. However, existing research seldom provides systematic analysis regarding subsequent local rolling reinforcement specifically applied to already rolled threads. Therefore, revealing the mechanism by which rolling reinforcement affects the surface evolution and fatigue performance at the thread root of pre-rolled bolts holds significant theoretical and engineering importance.

This paper focuses on 42CrMo high-strength bolts with rolled threads, investigating a local rolling reinforcement process at the thread root aimed at further enhancing their fatigue performance. The effects of rolling reinforcement were systematically evaluated by characterizing the surface integrity—including cross-sectional microstructure, surface morphology and roughness, and microhardness distribution—under different reinforcement parameters. Subsequently, high-frequency fatigue tests were conducted on specimens processed with different parameters. Fractographic analysis was combined to discuss the strengthening mechanism of rolling reinforcement from the perspective of fatigue fracture

mechanisms. This work aims to provide process guidance and a theoretical basis for the anti-fatigue manufacturing of high-strength bolts.

2. Materials and Methods

2.1. Materials and Processing

The high-strength bolt material selected for this study was 42CrMo steel, the specific chemical composition of which is listed in Table 1. To ensure material consistency, all specimens were sourced from the same batch of cylindrical stock measuring ϕ 100 mm × 600 mm. The stock was first processed via wire electrical discharge machining (EDM) into round bar specimens of ϕ 15 mm × 150 mm, followed by quenching and tempering heat treatment. The heat treatment process consisted of austenitizing at 850 °C in a high-vacuum high-pressure gas quenching furnace, followed by tempering at 450 °C in a vacuum tempering furnace. This process yielded a final material hardness of 42 HRC, with the corresponding mechanical properties detailed in Table 2.

Table 1. Chemical composition of 42CrMoA steel (wt./%).

C	Si	Mn	P	S	Cr	Ni	Cu	Mo	Als	W	V	Ti
0.42	0.19	0.64	0.016	0.004	1.04	0.02	0.01	0.169	0.018	0.001	0.006	0.006

Table 2. Mechanical properties of 42CrMoA steel.

Young's Modulus (GPa)	Yield Strength (MPa)	Tensile Strength (MPa)	Elongation (%)
244.42	>1270	>1390	7.8

Subsequently, the heat-treated samples were machined by turning to a final shank diameter of 10.8 mm in preparation for thread rolling. The threading was performed using a two-die radial infeed process with a rotational speed of 500 rpm and an applied pressure of 0.8 MPa. A dimensional drawing of the machined bolt specimen and a photograph of the finished rolled-thread bolt are presented in Figure 1.

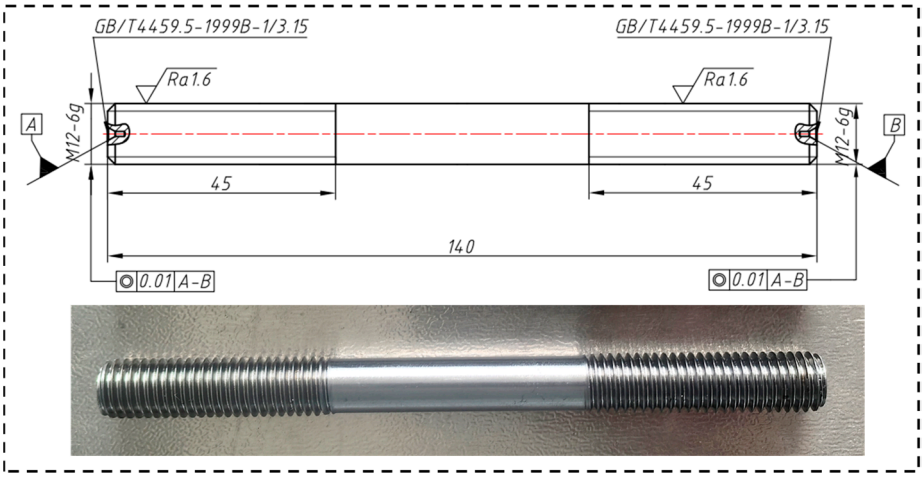


Figure 1. Specimen size diagram and molding specimen.

2.2. Experimental Scheme

Localized rolling reinforcement at the thread root of the rolled-thread bolts was performed using a dedicated thread rolling apparatus (model: RTIM-1, the fillet radius of the roller is 0.3 mm, as illustrated in Figure 2, China). To investigate the influence of different

rolling forces on the fatigue performance and elucidate the underlying mechanisms, three distinct rolling force levels were designed for the experimental campaign. This approach aimed to determine the optimal process parameter for maximizing fatigue life. The specific rolling force parameters implemented are detailed in Table 3.

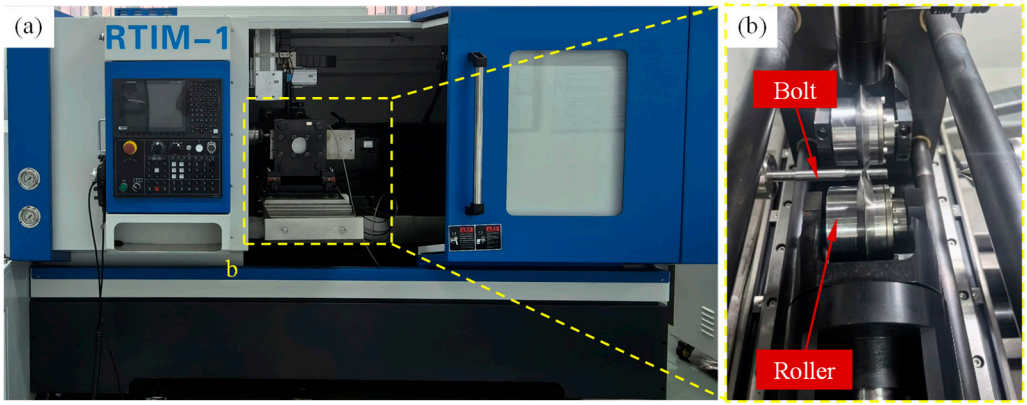


Figure 2. Dedicated thread rolling apparatus: (**a**) Overall view of the equipment. (**b**) Internal setting.

Table 3. Experimental parameters of thread rolling strengthening.

Number	Rolling Parameters
US	/
RS-2.5	2.5 kN
RS-3.5	3.5 kN
RS-4.5	4.5 kN

Tension–tension fatigue tests were conducted on both untreated (US) and root-rolled (RS) specimens using a high-frequency fatigue testing machine (model: GPS100, China). A custom-designed fixture for bolt fatigue testing, as shown in Figure 3b, was employed. The tests were run at the specimen's natural resonance frequency of 88 Hz. The maximum applied tensile stress was set at 850 MPa with a stress ratio (R) of 0.1. A step-loading procedure was adopted: if a specimen did not fail after 10^7 (10 million) cycles at 850 MPa, the stress amplitude was increased to 900 MPa for the subsequent test block, and this process was repeated iteratively.

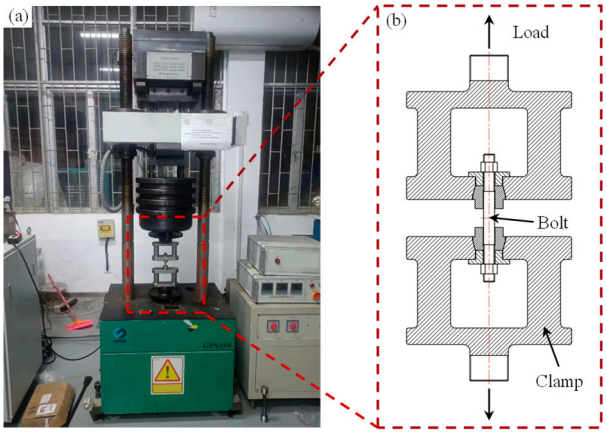


Figure 3. Tension–tension fatigue test: (**a**) High-frequency fatigue testing machine. (**b**) Bolt clamps.

2.3. Microstructure Characterization

Following fatigue testing, cross-sectional samples for microstructural analysis were prepared. Eight threads from the reinforced region were sectioned radially using wire electrical discharge machining (EDM, China). The sectioned halves were then mounted, and their surfaces were progressively ground with metallographic abrasive paper (from 180# to 2000# grit) and polished to a mirror finish. The polished samples were etched with a 4% nitric acid alcohol solution until the surface changed from metallic luster to a gray appearance for microstructural observation. The surface topography and roughness at the thread root were measured using a laser scanning confocal microscope (VK-X1000K, Japan). The near-surface microhardness at the thread root of the mounted samples was measured using a Vickers microhardness tester (FALCON-511, Holland) with a load of 200 gf and a dwell time of 10 s. A hardness profile was obtained by collecting data points at intervals of 50 μm along the radial direction from the surface into the core. The fatigue fracture morphology of both unreinforced and reinforced samples under identical loading conditions was observed and analyzed using a ZEISS Crossbeam 550 scanning electron microscope (SEM, Germany).

3. Results

3.1. Microscopic Structure

Figure 4 presents the cross-sectional microstructures at the thread root of the tested samples. Figure 4(a1) displays the typical metallographic features of the bolt after thread rolling, where grains near the thread root surface are aligned in a flow-line pattern along the rolling direction [21,22]. A magnified view of this region (Figure 4(a2)) reveals a distinct boundary of this flow-line structure, with a measured thickness of approximately 35.94 μm. The microstructural evolution after reinforcement with different rolling forces is shown in Figure 4(b1–d1). As the rolling force increases, the depth of the surface flow-line layer progressively expands. The corresponding magnified views (Figure 4(b2–d2)) indicate that the thickness of the flow-line layer increases to 79.53 μm, 87.54 μm, and 88.81 μm, respectively. Electron backscatter diffraction (EBSD) analysis was performed on a local area in Figure 4(d1). The inverse pole figure (IPF) map demonstrates that the rolling reinforcement at the thread root leads to further grain refinement in the surface layer and a more uniform distribution of grain size along the depth direction. However, some micro-defects are still discernible in the magnified images. Due to their random occurrence and size distribution, only qualitative analysis is performed on them in this study. These likely originate from the high surface hardness and reduced material toughness after thread rolling, which increases brittleness and may induce microscopic damage during the subsequent rolling process. Such defects may serve as potential initiation sites for fatigue cracks. Therefore, when evaluating the effect of rolling reinforcement on the fatigue performance of rolled-thread bolts, it is necessary to comprehensively consider the beneficial effect of increased flow-line layer depth against the potential detrimental influence introduced by micro-defects.

Figure 5 presents the EBSD analysis results for the thread root region of each sample. Figure 5(a1) shows the inverse pole figure (IPF) map of the US sample. A grain refinement layer is observable in the surface region resulting from the thread rolling process; however, its thickness is limited due to the nature of the bulk forming operation. The application of localized rolling reinforcement at the thread root significantly increases the depth of this refinement layer, as shown in Figure 5(b1–d1), and induces further grain refinement. The statistical results of grain size distribution within the scanned areas are presented in Figure 5(a2–d2). The minimum grain size in the US sample is approximately 0.80 μm. After rolling reinforcement, the minimum grain size decreases, reaching 0.74 μm in the RS-4.5 sample. Grain refinement increases the number of grain boundaries, which can effectively

hinder the formation and propagation of slip bands, thereby delaying the initiation of fatigue cracks. Furthermore, the kernel average misorientation (KAM) is positively correlated with dislocation density and can be used to analyze local strain and dislocation distribution [23,24]. The KAM distribution maps for each sample are shown in Figure 5(a3–d3), indicating a more consistent grain orientation in the surface layer of the thread root after rolling reinforcement. Statistical analysis of the local KAM values (Figure 5(a4–d4)) reveals that the average KAM values for the RS-2.5 and RS-4.5 samples are lower than that of the US sample, whereas the average KAM value for the RS-3.5 sample is higher. When the roller burnishing force is relatively small, plastic deformation is mainly concentrated in the material's surface layer, causing the orientation of surface grains to become more uniform, which leads to a decrease in the average KAM value and a corresponding reduction in dislocation density. As the roller burnishing force increases, the influence of plastic deformation extends to the subsurface layer, intensifying lattice distortion and promoting significant dislocation multiplication, thereby markedly increasing dislocation density. When the roller burnishing force is further increased, intense plastic deformation reorients the grain distribution in the subsurface layer, gradually aligning it with the orientation of surface grains. This results in the reorganization and annihilation of internal dislocation structures, leading to a decrease in dislocation density in this region. Meanwhile, the increase in dislocation density within the material helps hinder crack propagation, thus enhancing fatigue performance.

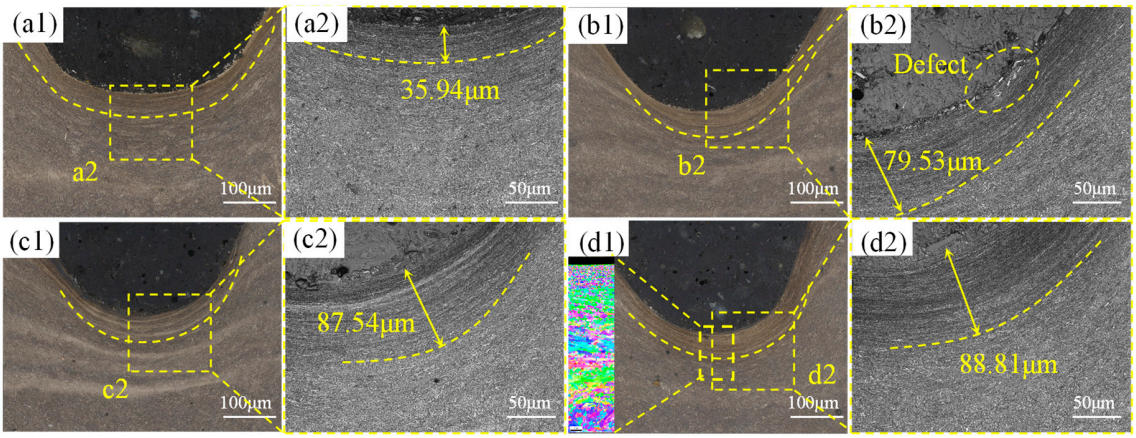


Figure 4. Microstructure of the thread root cross-section: (**a1–d1**) Microstructure images of the thread root cross-section for the US, RS-2.5, RS-3.5, and RS-4.5 samples, respectively. (**a2–d2**) Magnified views of the corresponding areas for each sample.

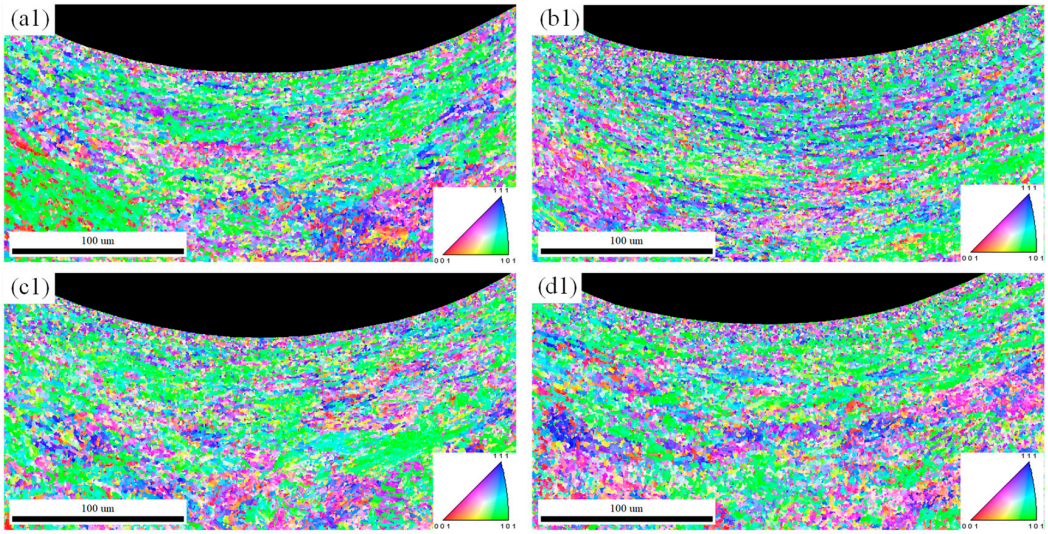


Figure 5. *Cont.*

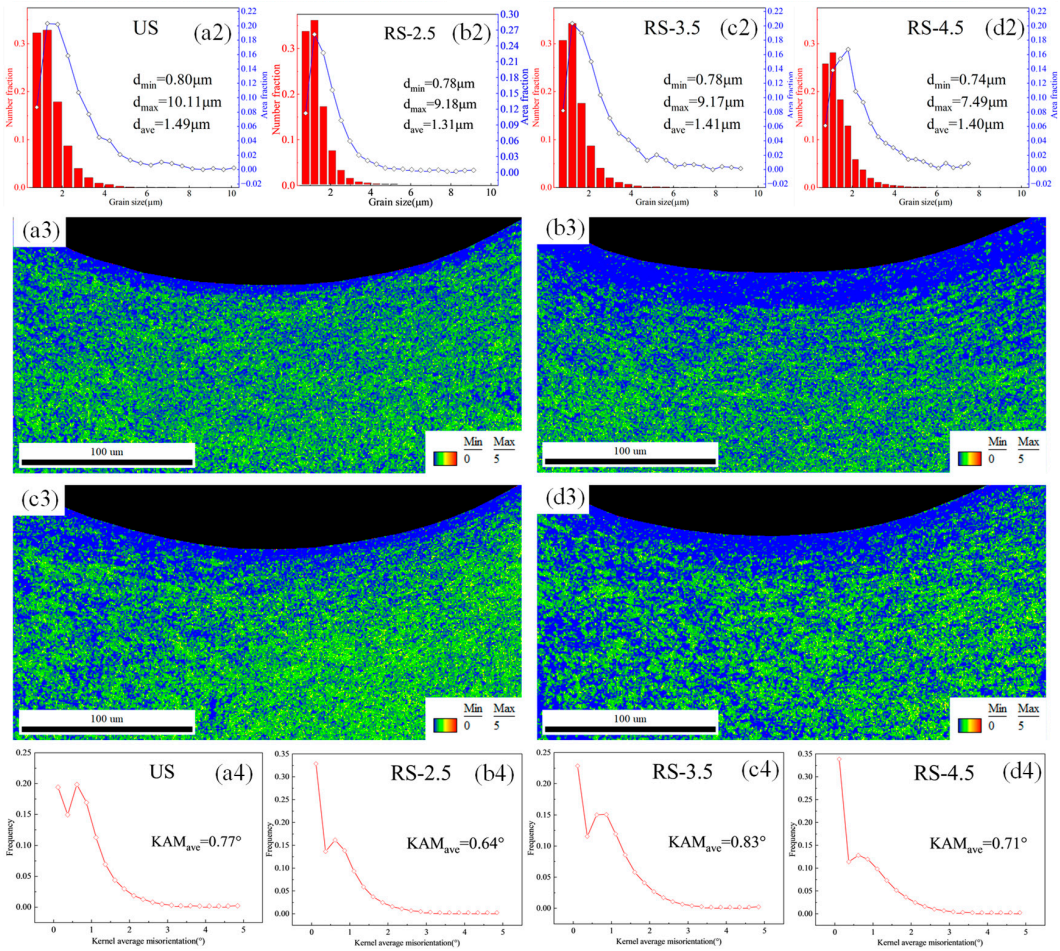


Figure 5. EBSD analysis of the samples: (**a1**–**d1**) IPF maps for the US, RS-2.5, RS-3.5, and RS-4.5 samples, respectively; (**a2**–**d2**) statistical grain size distribution maps for each sample; (**a3**–**d3**) KAM maps for each sample; (**a4**–**d4**) statistical KAM distribution maps for each sample.

3.2. Surface Morphology and Roughness

Figure 6 shows the surface morphology at the thread root of each sample. For bolts formed by thread rolling, the root morphology is primarily determined by the geometry of the rolling tool. As seen in Figure 6a for the US sample, although the rolling process improves surface finish to some extent, distinct machining marks along the processing direction are still visible on the thread root. This indicates that conventional thread rolling has a limited effect on suppressing such processing traces. After localized rolling reinforcement, the surface morphology of the sample roots changes significantly (Figure 6b–d). With increasing rolling force, the original machining marks gradually diminish and are replaced by more uniform rolling marks. The reduction in such surface defects helps to decrease stress concentration and delay the initiation of fatigue cracks, thereby playing a crucial role in enhancing the overall fatigue performance of the bolts [25,26].

Figure 7 shows the surface roughness measurements taken at the thread root of each sample for the quantitative evaluation of surface quality. The surface roughness of the RS samples exhibits an increasing trend with higher rolling force. Compared to the US sample, the variation in surface roughness after reinforcement ranges from −43% to 26%. Due to the relatively good initial surface quality of the US sample, the subsequent rolling reinforcement results in a fluctuating effect on roughness, influenced by the magnitude of the rolling force. The results indicate that properly controlling the rolling force is a critical factor in regulating the surface morphology and roughness of the threads, both of which directly affect the fatigue performance of the material. When the rolling force is insufficient,

the reinforcement effect is limited, making it difficult to effectively eliminate the original machining marks. Conversely, excessively high rolling force may compromise the existing surface integrity and lead to increased roughness. Therefore, optimizing the rolling force is essential for achieving a superior surface condition beyond the baseline thread-rolled state.

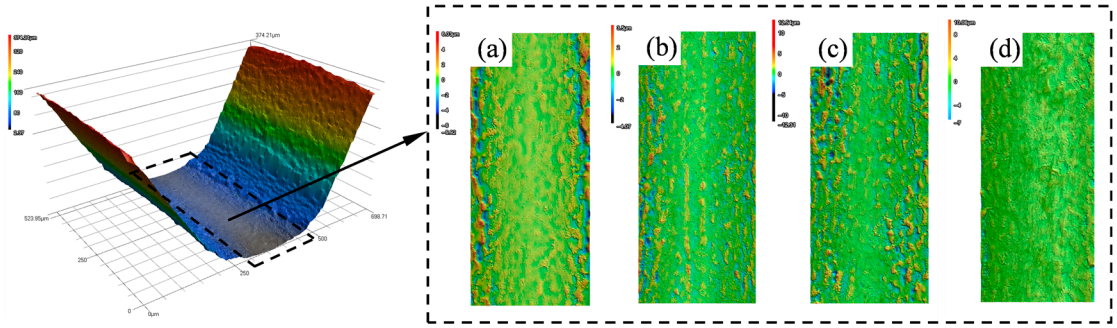


Figure 6. Surface morphology at the thread root: (**a**) US, (**b**) RS-2.5, (**c**) RS-3.5, (**d**) RS-4.5.

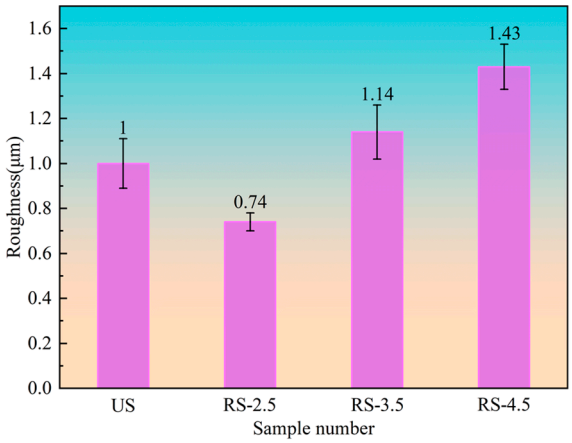


Figure 7. Surface roughness at the thread root.

3.3. Microhardness Distribution

Figure 8 presents the microhardness distribution fields mapped from cross-sectional measurements of each sample. As shown in Figure 8a, the surface hardness of the US sample produced by thread rolling is approximately 500 $HV_{0.2}$, significantly higher than the core hardness (~420 $HV_{0.2}$), which results from the plastic deformation induced at the surface during the rolling process. Within the core region at depths of 0.4–1 mm, the hardness distribution is inhomogeneous along the axial direction. The hardness distributions after applying rolling reinforcement with different parameters are shown in Figure 8b–d. For the RS-2.5 sample, the surface hardness increases to about 540 $HV_{0.2}$. However, the depth of the hardness gradient remains similar to that of the US sample, converging toward the matrix hardness at approximately 100 μm below the surface. Additionally, the hardness distribution in the core becomes more uniform along the axial direction. With an increase in rolling force, the surface hardness of the RS-3.5 sample (Figure 8c) does not show further enhancement; in fact, localized regions exhibit a decrease. Nevertheless, the depth of the hardness gradient extends to about 180 μm. Excessive rolling force, as in the RS-4.5 sample (Figure 8d), may introduce surface defects, reduce the deformation resistance of the surface material, and consequently lead to a drop in hardness. Changes in material hardness indirectly reflect variations in strength, with higher hardness generally corresponding to increased tensile and yield strength. Localized rolling reinforcement at the thread root effectively enhances both surface hardness and the depth of the hardness gradient, thereby contributing to the retardation of fatigue crack initiation [27,28].

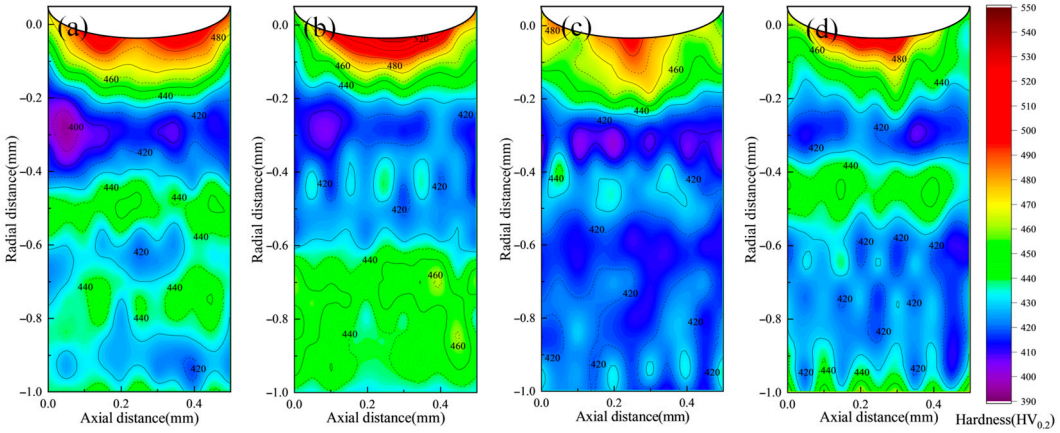


Figure 8. Microhardness distribution fields: (**a**) US sample, (**b**) RS-2.5 sample, (**c**) RS-3.5 sample, (**d**) RS-4.5 sample.

3.4. Fatigue Life

Figure 9 presents a comparison of the fatigue life for each sample under identical high-frequency fatigue testing parameters, with the specific lifetime data provided in Table 4. The RS-4.5 sample could not undergo fatigue testing due to excessive deformation, which prevented its assembly with a standard nut. Compared to the US sample, the specimens subjected to thread root rolling reinforcement exhibited a significant improvement in fatigue life. The average fatigue life of the RS-2.5 sample was approximately 2.7 times that of the US sample. Under the same testing conditions, the RS-3.5 sample achieved a fatigue life of up to 10^7 cycles, representing an approximately 11-fold increase relative to the US sample. For the US samples, the coefficient of variation (CV) of their fatigue life was 27.1%, which falls within the normal range of dispersion for material fatigue testing. After rolling strengthening, the CV value of the RS-2.5 specimens further decreased to 20.9%, indicating that the process not only improved fatigue life but also significantly enhanced the stability of performance, reflecting the beneficial effect of rolling on material uniformity. However, the CV value of the RS-3.5 specimens increased significantly. This is primarily attributed to one specimen exhibiting exceptionally high fatigue life (reaching 10^7 cycles without failure). This result suggests that the current process parameters are capable of unlocking the material's ultra-high fatigue potential, but it also indicates that the stability still requires improvement, possibly due to sensitivity to microstructure or local defects. Therefore, there remains room for further optimization and control of this process condition. Future work should systematically investigate the sources of variation to achieve a balance between high fatigue life and high stability. The results demonstrate that implementing localized rolling reinforcement at the bolt root following thread rolling can effectively enhance fatigue life.

Table 4. Fatigue life data of the tested samples.

Number	Fatigue Life (Cycles)			Average Life (Cycles)
US	388,547	551,571	681,160	540,426
RS-2.5	1,803,317	1,355,234	1,222,062	1,460,204
RS-3.5	10^7 run-out (950 MPa: 577,694)	5,131,310	2,868,273	5,999,861

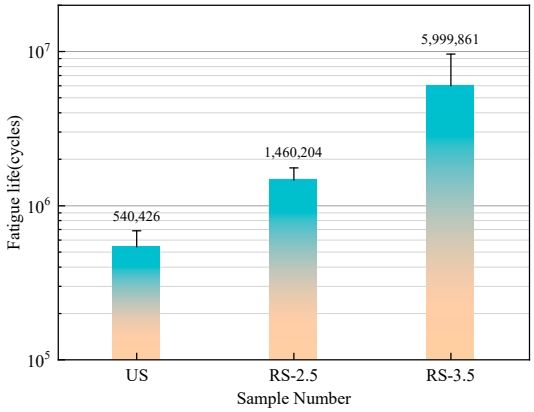


Figure 9. Comparison of fatigue life among the tested samples (bar chart).

3.5. Fatigue Fracture Characteristics

Figure 10 presents the macroscopic fracture morphology of each sample under identical fatigue loading. After high-frequency fatigue testing, the fractures of all specimens exhibit the three characteristic regions typical of fatigue failure [29,30]: the fatigue crack initiation zone (Region I), the fatigue crack propagation zone (Region II), and the final overload fracture zone (Region III), as shown in Figure 10(a1,b1,c1). For the US specimen formed solely by thread rolling, the combination of high stress concentration at the thread root and the relatively shallow deformation layer induced by the forming process results in a multi-site crack initiation feature, as seen in Figure 10(a1). The application of localized rolling reinforcement to the thread root enhances the surface material strength and increases the depth of the deformed layer, thereby effectively suppressing surface crack initiation. As shown in Figure 10(b1,c1), with increasing rolling force, the number of crack initiation sites decreases, and the fracture mode transitions progressively from multi-site to single-site initiation. Typical fatigue striations are observable within the crack propagation zone (Region II). These striations form due to the cyclic opening and closing of the crack tip under alternating loading, resulting in uniformly spaced bands. The normal direction to these striations (indicated by the red arrows in Figure 10(a2,b2,c2)) represents the local crack growth direction. When the crack extends to a critical size, unstable propagation occurs, leading to instantaneous specimen failure, which corresponds to Region III in the fracture surfaces. Magnified views of the crack initiation zones for each specimen are provided in Figure 10(a3,b3,c3), revealing that in all cases, cracks originated from surface discontinuities such as machining marks.

Based on the comprehensive observation of fatigue fracture characteristics, the mechanism by which the strengthening layer influences fatigue performance is elaborated. Local rolling strengthening affects the properties of both the surface and subsurface layers. Since the location of the primary fatigue origin did not change significantly before and after rolling—indicating that fatigue initiation consistently originated from discontinuous tool marks—it reveals that changes in surface properties (i.e., surface roughness and surface hardness) had a limited impact on fatigue performance in this study. The improvement in fatigue performance is instead attributed to the enhancement of subsurface layer properties. For instance, as the rolling force increases, greater plastic deformation induces microstructural changes, such as local grain refinement. This aligns with the findings of Krbata et al. [31], who demonstrated the influence of plastic deformation on microstructure by comparing deformation continuous cooling transformation (DCCT) diagrams with conventional continuous cooling transformation (CCT) diagrams. The improvement in subsurface properties is also reflected in the hardness gradient, with rolling strengthening producing a deeper hardened gradient layer. The enhancement of subsurface properties

effectively suppresses the initiation and propagation of secondary fatigue origins. This is most clearly observed on the fracture surfaces as a reduction in the number of fatigue origins, thereby delaying the overall fracture process and ultimately extending the fatigue life of the bolts.

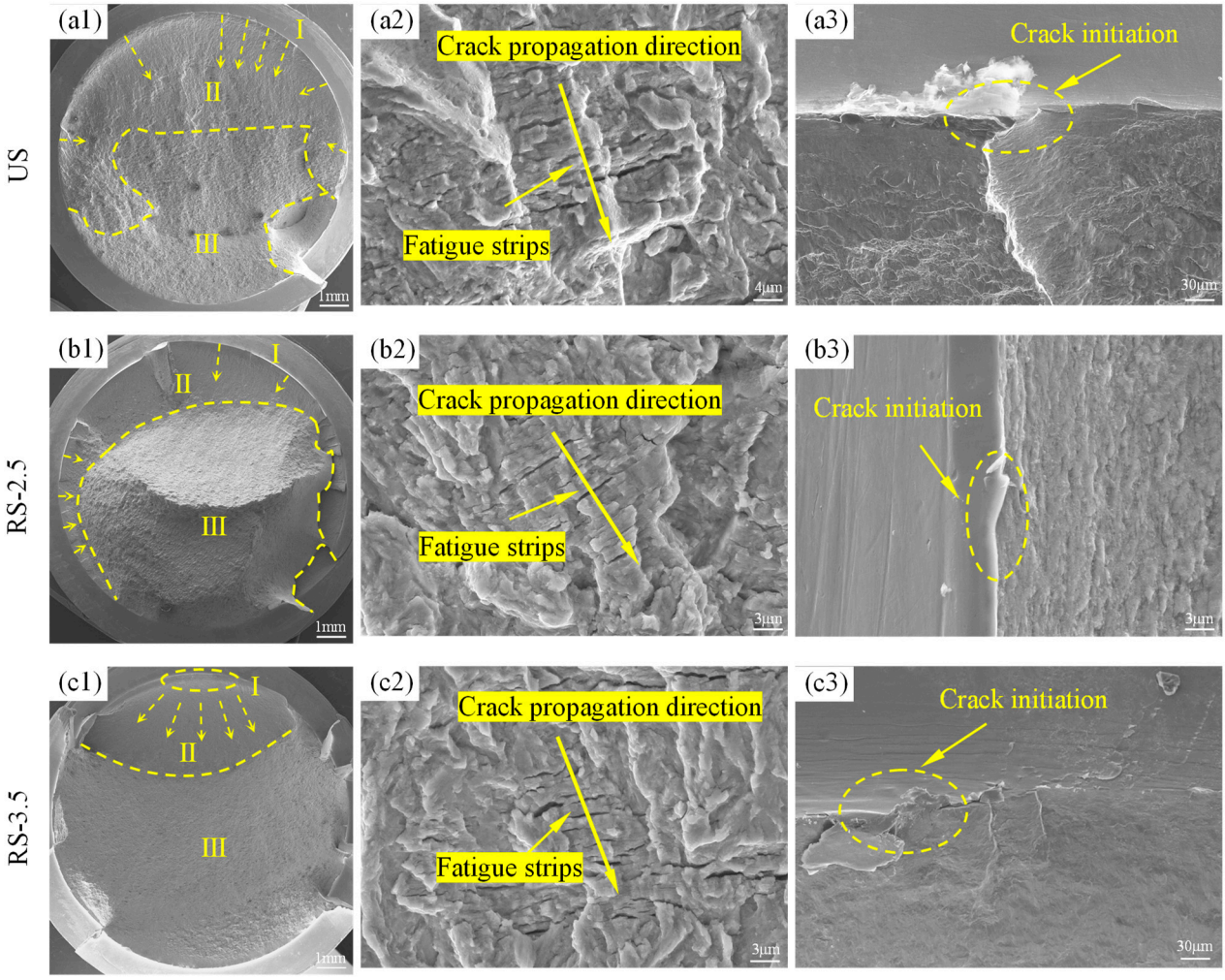


Figure 10. Fracture morphology of the samples after fatigue testing (R = 0.1, σ_{max} = 850 MPa): (**a1**–**a3**) US sample (life: 388,547 cycles); (**b1**–**b3**) RS-2.5 sample (life: 1,355,234 cycles); (**c1**–**c3**) RS-3.5 sample (life: 107 cycles run-out).

4. Conclusions

This study systematically elucidates the influence mechanism of thread root rolling reinforcement on the surface properties of rolled-thread bolts. The main conclusions are as follows:

(1) The rolling reinforcement treatment significantly alters the near-surface characteristics at the thread root. Post-reinforcement, the depth of the grain refinement layer increases from an initial 35.94 μm to 87.54 μm. Accompanied by further grain refinement and an increase in dislocation density, the depth of the affected microhardness layer extends from approximately 100 μm to 180 μm. The synergistic effect of these microstructural optimizations results in an approximately 11-fold enhancement in the fatigue life of the bolts.

(2) Systematic analysis of the fatigue fracture surfaces reveals that rolling reinforcement effectively improves the surface integrity of the thread root, reducing surface defects. This directly leads to a significant decrease in the number of crack initiation sites. The most pronounced manifestation of this improvement is the transition in fatigue fracture mode

from multiple origins in the unreinforced state to a fracture dominated by a single crack initiation site.

Future work will consider methods for measuring the residual stress field at the thread root to quantify its specific contribution to fatigue performance enhancement. When performing rolling strengthening on the thread root, the degree of plastic deformation must be strictly controlled to avoid affecting assembly fit due to thread dimensional deviations. This is also one of the limitations that need to be emphasized in the current practical application of this technology.

Author Contributions: Z.H.: writing—original draft, investigation, formal analysis. S.C.: writing—review & editing, supervision. Z.X.: methodology, data curation, project administration. F.Z.: resources, methodology. Z.L.: software, visualization. W.C.: validation, investigation. Q.J.: validation, funding acquisition. B.G.: methodology, conceptualization. All authors have read and agreed to the published version of the manuscript.

Funding: This research was funded by the National Natural Science Foundation of China [No. 52475459], the Science and Technology Project of Fujian Province, China [No. 2022HZ024009, 2021HZ024006], Fujian Marine Equipment Anti-fatigue Manufacturing Engineering Research Center, in China [No. Z823291], the Major Science and Technology Project of Xiamen, Fujian, China [No. 3502Z20231011], and the Research Project on Manufacturing Technology for Long-Life Fatigue Resistant Connecting Pins of Xiamen, Fujian, China [No. 2024350204006292], and the Natural Science Foundation of Xiamen City, China [No. 3502Z202372025].

Data Availability Statement: Data will be made available on request.

Conflicts of Interest: Author Fasheng Zhong was employed by the company Xiamen XGMA CREC Heavy Machinery Co. The remaining authors declare that the research was conducted in the absence of any commercial or financial relationships that could be construed as a potential conflict of interest.

References

1. Sun, H.; Dong, J.; Liu, H.; Shi, W.; Feng, Q.; Yao, K.; Huang, S.; Peng, L.; Cai, Z. Review of non-destructive testing for wind turbine bolts. *Sensors* **2025**, *25*, 5726. [CrossRef]
2. Tao, T.; Yang, Y.; Yang, T.; Liu, S.; Guo, X.; Wang, H.; Liu, Z.; Chen, W.; Liang, C.; Long, K.; et al. Time-domain fatigue damage assessment for wind turbine tower bolts under yaw optimization control at offshore wind farm. *Ocean Eng.* **2024**, *303*, 117706. [CrossRef]
3. Liu, N.; Cui, X.; Xiao, J.; Lua, J.; Phan, N. A simplified continuum damage mechanics based modeling strategy for cumulative fatigue damage assessment of metallic bolted joints. *Int. J. Fatigue* **2020**, *131*, 105302. [CrossRef]
4. Shen, X.; Lu, L.; Zeng, D. Fatigue failure analysis of high strength bolts used for high-speed railway vehicle braking discs. *Eng. Fail. Anal.* **2020**, *115*, 104661. [CrossRef]
5. Abdul Jawwad, A.K.; Alshabatat, N.; Mahdi, M. The effects of joint design, bolting procedure and load eccentricity on fatigue failure characteristics of high-strength steel bolts. *Eng. Fail. Anal.* **2021**, *122*, 105279. [CrossRef]
6. Jiao, J.; Liu, Z.; Guo, Q.; Liu, Y.; Lei, H. Constant-amplitude fatigue behavior of m24 high-strength bolt of end-plate flange connection. *Structures* **2021**, *34*, 2041–2053. [CrossRef]
7. Zhang, D.; Li, D.; Liu, B.; Yu, Z.; Zhao, S. Investigation and implementation for forming lead screw by through-feed rolling process with active rotation. *J. Manuf. Process.* **2022**, *82*, 96–112. [CrossRef]
8. Du Maire, P.; Hoffmeister, J.; Johlitz, M.; Öchsner, A. Influence of the manufacturing process on the fatigue strength of threads. *Materwiss. Werksttech.* **2025**, *56*, 638–645. [CrossRef]
9. Zhang, S.; Zhang, D.; Jiang, H.; Jiang, F.; Zhao, S. Numerical and experimental analysis of deformation behaviors and microstructure evolution in the thread rolling process. *J. Mater. Res. Technol.* **2022**, *19*, 230–242. [CrossRef]
10. Zhou, J.; Li, L.; Hang, P.; Ding, Y. Effects of heat treatment and thread rolling sequence on fatigue and corrosion resistance of 304/q235 bimetal composite bolts. *Mater. Today Commun.* **2025**, *45*, 112175. [CrossRef]
11. Jiang, F.; Zhao, S.; Zhang, S.; Gao, J.; Jiang, H.; Fei, L. Finite element analysis and experiment study on axial infeed hot rolling process of thread with ti6al4v. *Int. J. Adv. Manuf. Technol.* **2022**, *121*, 5873–5884. [CrossRef]
12. Wang, W.; Bai, L.; Shi, D.; Jin, H.; Yang, Y.; Su, K.; Mei, Q. Evolution of graded surface microstructure and property of ti6al4v threads processed by surface rolling. *Metals* **2024**, *14*, 1189. [CrossRef]

13. Zhang, S.; Zhang, D.; Zhao, S.; Jiang, F.; Lee, M. Characteristics of surface and subsurface of formed thread parts by axial-infeed thread rolling process. *Chin. J. Aeronaut.* **2023**, *36*, 471–481. [CrossRef]
14. Lu, Y.; Hu, L.; Li, T.; Ran, G.; Yi, X.; Sun, Y.; Kong, Z.; Yan, K.; Hu, R.; Wang, H. High cycle fatigue performance and corresponding fracture behaviors of gh4169 studs formed by thread warm rolling process. *Int. J. Fatigue* **2025**, *193*, 108808. [CrossRef]
15. Wang, R.; Zhang, X.; He, P.; Wang, W.; Chen, W.; Wei, X.; Pan, X.; Zhou, L. Femtosecond laser shock peening of ultra-thin-walled ti-6al-4v: Study on surface integrity and high cycle fatigue mechanism. *J. Mater. Res. Technol.* **2025**, *37*, 4136–4152. [CrossRef]
16. Wu, J.; Zuo, Z.; Geng, J.; Wang, Z.; Dang, J.; Li, Y.; Zhang, C.; Chen, D.; Chen, M.; Wang, H. The effects of stress ultrasonic rolling on the surface integrity and fatigue properties of tib2/7050 al composite. *J. Manuf. Process.* **2024**, *118*, 315–330. [CrossRef]
17. Zhang, Y.; Jian, X.; Xia, F.; Shi, D.; Wu, L.; Liu, L.; Ji, V. Effect of laser shock peening on surface integrity and tensile fatigue behavior of tb8 bolts. *Eng. Fail. Anal.* **2024**, *157*, 107968. [CrossRef]
18. Wang, X.; Xiong, X.; Huang, K.; Ying, S.; Tang, M.; Qu, X.; Ji, W.; Qian, C.; Cai, Z. Effects of deep rolling on the microstructure modification and fatigue life of 35cr2ni4moa bolt threads. *Metals* **2022**, *12*, 1224. [CrossRef]
19. Cheng, M.; Zhang, D.; Chen, H.; Qin, W. Development of ultrasonic thread root rolling technology for prolonging the fatigue performance of high strength thread. *J. Mater. Process. Technol.* **2014**, *214*, 2395–2401. [CrossRef]
20. Wang, D.; Lu, X.; Zhao, J.; Lin, H.; Zhang, M. Study on the effect of Rolling Strengthening on the Surface Integrity of 45 Steel Thread root. *J. Mech. Strength* **2022**, *44*, 1075–1081. [CrossRef]
21. Zhu, W.; Wang, D.; Cheng, P.; Shao, C.; Zhang, P.; Li, L.; Wang, Y. Evolution of surface morphology and microstructure in reactor pressure vessel studs during triaxial rolling. *Int. J. Adv. Manuf. Technol.* **2023**, *126*, 4591–4605. [CrossRef]
22. Aktas, S.; Kisioglu, Y. Effects of thread rolling processing parameters on mechanical properties and microstructures of high-strength bolts. *Mater. Test.* **2020**, *62*, 1017–1024. [CrossRef]
23. Liu, L.; Li, L.; Kang, H.; Xu, G.; Ma, Y.; Zhao, M.; Chen, Z.; Liu, Z. Enhancing the surface integrity and high-stress-concentration notched fatigue performance of 18crnimo7-6 carburized steel via ultrasonic surface rolling. *Mater. Sci. Eng. A* **2026**, *952*, 149629. [CrossRef]
24. Wang, H.; Wang, X.; Hu, X.; Tian, Y. Study on the micro-mechanism of ultrasonic rolling strengthening of quenched 42crmo steel. *Met. Mater.-Int.* **2025**, *31*, 3808–3823. [CrossRef]
25. Zhou, Y.; Chu, X.; Sun, J.; Han, R.; Sun, X. Improved surface integrity and fatigue property of fv520b steel via surface mechanical rolling treatment process. *Mater. Sci. Eng. A* **2025**, *923*, 147708. [CrossRef]
26. Luan, X.; Zhao, W.; Liang, Z.; Xiao, S.; Liang, G.; Chen, Y.; Zou, S.; Wang, X. Experimental study on surface integrity of ultra-high-strength steel by ultrasonic hot rolling surface strengthening. *Surf. Coat. Technol.* **2020**, *392*, 125745. [CrossRef]
27. Deng, J.; Shen, Z.; Huang, Z.; Su, Y. Effect of static pressure during ultrasonic surface rolling process on surface integrity and fatigue performance of a die-forged 2014 aluminum alloy aircraft wheel. *Mater. Today Commun.* **2025**, *49*, 114170. [CrossRef]
28. Gong, B.S.; Zhang, Z.J.; Wang, H.W.; Liu, R.; Liu, H.Z.; Wang, H.; Purcek, G.; Demirtas, M.; Yanar, H.; Zhang, Z.F. A novel surface strengthening technique for enhancing fatigue properties of 6061 al alloy. *Int. J. Fatigue* **2025**, *198*, 109000. [CrossRef]
29. Zhao, W.; Liu, D.; Shi, H.; Hao, Z.; Zhao, J. The effect of surface gradient nanostructure and compressive residual stress on fretting fatigue of a100 ultra-high strength steel by ultrasonic surface rolling process. *Int. J. Fatigue* **2025**, *193*, 108775. [CrossRef]
30. Liu, H.; Kang, R.; Zhu, X.; Dong, Z.; Xu, Z.; Song, Y. Study on the effect of surface rolling process on fatigue behavior and surface integrity of 300m steel thread root. *J. Mater. Res. Technol.* **2025**, *38*, 5996–6010. [CrossRef]
31. Krbata, M.; Krizan, D.; Eckert, M.; Kaar, S.; Dubec, A.; Ciger, R. Austenite Decomposition of a Lean Medium Mn Steel Suitable for Quenching and Partitioning Process: Comparison of CCT and DCCT Diagram and Their Microstructural Changes. *Materials* **2022**, *15*, 1753. [CrossRef] [PubMed]

Disclaimer/Publisher's Note: The statements, opinions and data contained in all publications are solely those of the individual author(s) and contributor(s) and not of MDPI and/or the editor(s). MDPI and/or the editor(s) disclaim responsibility for any injury to people or property resulting from any ideas, methods, instructions or products referred to in the content.